Path following for an autonomous paraglider

Chiara Toglia   Marilena Vendittelli   Leonardo Lanari

Abstract— This paper addresses the path following problem for an autonomous parafoil-payload system. The actuated dynamics of the system is first detailed. Local exponential stability of an input-output feedback linearizing control is proved, achieving a stable line following in the XY plane by using only lateral directional control input.

I. INTRODUCTION

Parafoil-payload systems (aka paragliders) represent a potential light, low cost, space efficient mean for autonomous transportation. They can be used for accurate delivering of payloads using inexpensive guidance and control modules to inaccessible areas, as in natural disasters response. If equipped with proper sensors, it is possible to perform scientific observations during flight. Aerial remote sensing or video servoing of the surface can also be carried out. Finally, tethered airfoils can also be used for wind energy generation at high altitude [1].

The study of parafoil-payload systems started in the mid 60's. A planar dynamics, linearized for relatively small deflections, is detailed in [2], along with a stability analysis of longitudinal dynamics during vertical descent. In [3] a tridimensional multibody 10 degrees of freedom (DOF) model is presented, with a procedure for investigating the small-disturbance stability of a freely descending nonrigid parachute. A wide literature is related to the aerodynamics acting on the paraglider. Apparent forces and moments of the surrounding air act on such a light structure, as shown in [4]. Aerodynamic forces and moments can be computed using proper coefficients which depend on the canopy (dimension, shape of the profile, etc.). Schroeder Iacomini and Cerimele developed a database for longitudinal and lateral directional aerodynamic, analyzing data collected during several large parafoil drop tests conducted by NASA [5], [6].

For a proper dynamical model, not only aerodynamics and gravity but several other aspects may be included, like canopy's changing shapes and aerodynamics or interaction between parafoil and payload. The model of the paraglider can be written using different number of DOF. For instance, since in the first approximation the longitudinal and lateral dynamics are decoupled, it is possible to have 3-DOF models to describe only the longitudinal [7] or lateral dynamics [8]. If a complete nonlinear model is considered, then the paraglider can be described as a 6-DOF rigid body [9]. More

advanced models consider the paraglider as a multibody system, thus the relative different attitude of parafoil and payload is studied by adding further DOF. Since the relative roll angle is negligible, several 8-DOF models are presented in literature [10], [11], [12]. To have a complete attitude dynamics of the parafoil and payload separately, [13] presents a 9-DOF model, together with an original aerodynamics model: the parafoil is modeled as a collection of joint panels on which only lift and drag act (no sideslip force, no rolling, pitching, yawing moments), showing that for small brake deflections only roll and skid steering are exhibited.

Despite the lively activity in modeling parafoil-payload systems, few results are available in control. Examples include [12], [14], which propose heuristic-based control law without providing any formal proof of convergence.

This paper presents preliminary results in the control of autonomous paragliders along a given path. In particular, a path following algorithm for straight lines on the ground, based on feedback linearization, is proposed. Straight lines are paths of interest for this system in view of the wide un-cluttered space in which they are suppose to move for long-range transportation tasks. To the best of our knowledge, this is the first control algorithm proposed in the literature for which a formal proof of convergence is provided.

In Sec. II we detail the 6-DOF model used in this paper, which is very similar to the model used in [9]. The control problem is formulated and solved in Sec. III, while in Sec. IV the proposed approach is validated through simulations.

II. MATHEMATICAL MODEL

The dynamics of the paraglider and payload system can be described using a 6-DOF model if the system is supposed to be rigid, thus neglecting the relative motion of parafoil and payload. The state vector is composed by the position of the center of mass (CM), see Fig. 1, $X_{CM} = [x, y, z]^T$ in the inertial reference frame, the Euler angles $[\varphi, \vartheta, \psi]^T$, the velocity of the CM in the body fixed reference frame $V_{cm} = [u, v, w]^T$ and the angular velocities $\omega = [p, q, r]^T$. The velocity of the CM can be described alternatively using the module $V_T = \sqrt{u^2 + v^2 + w^2}$, the angle of attack $\alpha = \tan^{-1}(w/u)$ and the sideslip angle $\beta = \sin^{-1}(v/V_T)$.

Introducing the rotation matrix from the body fixed to the inertial reference frame

$$T_{ib} = \begin{bmatrix} c_\vartheta c_\psi & s_\varphi s_\vartheta c_\psi - c_\varphi s_\psi & c_\varphi s_\vartheta c_\psi + s_\varphi s_\psi \\ c_\vartheta s_\psi & s_\varphi s_\vartheta s_\psi + c_\varphi c_\psi & c_\varphi s_\vartheta s_\psi - s_\varphi c_\psi \\ -s_\vartheta & s_\varphi c_\vartheta & c_\varphi c_\vartheta \end{bmatrix},$$

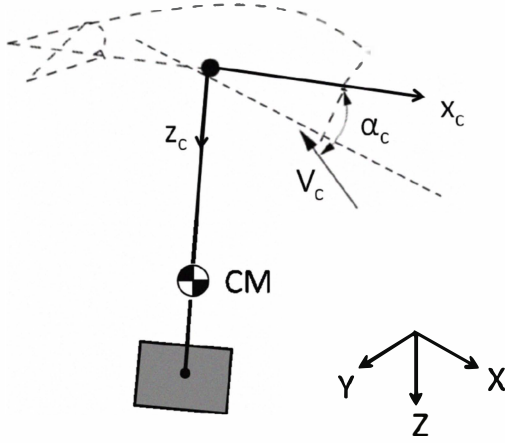the kinematic equations in terms of inertial position and Euler angles can be easily written as

Fig. 1. Schematic of parafoil and payload system

$$\dot{X}_{cm} = T_{ib}V_{cm} \tag{1}$$

$$\begin{bmatrix} \dot{\varphi} \\ \dot{\vartheta} \\ \dot{\psi} \end{bmatrix} = \begin{bmatrix} 1 & s_\varphi t_\vartheta & c_\varphi t_\vartheta \\ 0 & c_\varphi & -s_\varphi \\ 0 & s_\varphi/c_\vartheta & c_\varphi/c_\vartheta \end{bmatrix} \begin{bmatrix} p \\ q \\ r \end{bmatrix}.$$

The dynamics of the CM expressed in the body fixed reference frame is

$$Ma_{cm} = W + F_A^c + F_A^b + F_{app} \tag{2}$$

$$I\dot{\omega} = -\Omega I\omega + M_A^c + M_{app} + X_{gc} \wedge F_A^c +$$
$$+X_{gc} \wedge F_{app} + X_{gb} \wedge F_A^b$$

being M the mass matrix, Ω the skew-symmetric matrix of ω, W the weight force, F_A^c and F_A^b the aerodynamic forces acting on the canopy and the payload, M_A^c the aerodynamic moment, F_{app} and M_{app} the apparent force and moment, $X_{gc} \wedge F_A^c$, $X_{gb} \wedge F_A^b$ and $X_{gc} \wedge F_{app}$ the moments generated on the CM by the aerodynamics and apparent forces, X_{gc} and X_{gb} the vectors from the global to the canopy's and payload's CM. The acceleration a_{cm} of the CM is

$$a_{cm} = \dot{V}_{cm} + \omega \wedge V_{cm}. \tag{3}$$

Aerodynamic drag acts both on parafoil and payload, while only the parafoil is affected by lift. The aerodynamics also generates rolling, pitching and yawing moments:

$$F_A^b = -\frac{1}{2}\rho S_b \|V_b\| C_D^b V_b$$

$$F_A^c = \frac{1}{2}\rho S_c \|V_c\|^2 \begin{bmatrix} C_L s_{\alpha_c} c_{\beta_c} - C_D c_{\alpha_c} c_{\beta_c} \\ -C_D s_{\beta_c} \\ -C_L c_{\alpha_c} c_{\beta_c} - C_D s_{\alpha_c} c_{\beta_c} \end{bmatrix}$$

$$M_A^c = \frac{1}{2}\rho S_c \|V_c\|^2 \begin{bmatrix} \dfrac{C_{l_p}}{2\|V_c\|} b^2 p + C_{l_\varphi} b\varphi \\ \dfrac{C_{m_q}}{2\|V_c\|} c^2 q + C_m c \\ \dfrac{C_{n_r}}{2\|V_c\|} b^2 r \end{bmatrix}$$

where $V_c = V_{cm} + \omega \wedge X_{gc}$ and $V_b = V_{cm} + \omega \wedge X_{gb}$ are the parafoil and payload velocities, S_c and S_b are parafoil and

payload surfaces, b and c are the canopy's span and chord length. Aerodynamic coefficients depend on α:

$$C_L = C_{L_0} + C_{L_\alpha}\alpha \qquad C_D = C_{D_0} + C_{D_\alpha}\alpha^2$$
$$C_m = C_{m_0} + C_{m_\alpha}\alpha.$$

Apparent forces and moments act on the system since the air surrounding the parafoil creates an additional field of fluid momentum and energy due to its induced motion. Such effect was first introduced in the modeling analysis by Lissaman and Brown [4], providing analytical formulation to compute apparent mass M_F and moment of inertia I_F. F_{app} and M_{app} are:

$$F_{app} = -M_F a_{cm} - \omega \wedge M_F V_c \tag{4}$$
$$M_{app} = -I_F \dot{\omega} - \Omega I_F \omega - V_c \wedge M_F V_c.$$

Using eq. (3) and eq. (4) in eq. (2), one has:

$$(M + M_F)\dot{V}_{cm} = W + F_A^c + F_A^b - \Omega M_F V_c +$$
$$-(M + M_F)\Omega V_{cm} \tag{5}$$
$$R_{gc}M_F\dot{V}_{cm} + (I + I_F)\dot{\omega} = M_A^c - \Omega(I + I_F)\omega +$$
$$+R_{gc}(F_A^c - \Omega M_F V_c) + R_{gb}F_A^b - \Xi_c M_F V_c$$

where R_{gc}, R_{gb}, Ξ_c are the skew-symmetric matrices for the vectors X_{gc}, X_{gb} and V_c, respectively.

A. Effect of flaps deflection on the aerodynamics

Beside the angle of attack, the aerodynamic coefficients also depend on the flap deflection. The two flaps are located laterally on the parafoil's tail. If both are deflected of the same angle, an increase of lift and drag occurs, while the efficiency decreases. If the flaps deflection is asymmetric, a difference in drag between the two sides occurs, inducing rolling and yawing moments. In the lateral-directional dynamics the roll and yaw terms are coupled. After an initial transient, a constant turn rate is achieved when the moments are balanced by damping terms C_{l_φ}, C_{l_p} and C_{n_r}.

Introducing the symmetrical δ_s and asymmetrical δ_a flaps deflection, the control flap width t, the variation of forces ΔF_a^c and moments ΔM_a^c can be written as:

$$\begin{bmatrix} \Delta F_a^c \\ \Delta M_a^c \end{bmatrix} = \frac{1}{2}\rho S_c \|V_c\|^2 \begin{bmatrix} S_{F_a^c} \\ S_{M_a^c} \end{bmatrix} \begin{bmatrix} \delta_a \\ \delta_s \end{bmatrix} \tag{6}$$

being

$$S_{F_a^c} = \begin{bmatrix} 0 & C_{L_{\delta_s}} s_{\alpha_c} c_{\beta_c} - C_{D_{\delta_s}} c_{\alpha_c} c_{\beta_c} \\ 0 & -C_{D_{\delta_s}} s_{\beta_c} \\ 0 & -C_{L_{\delta_s}} s_{\alpha_c} c_{\beta_c} - C_{D_{\delta_s}} c_{\alpha_c} c_{\beta_c} \end{bmatrix}$$

$$S_{M_a^c} = \begin{bmatrix} C_{l_{\delta_a}} b/t & 0 \\ 0 & 0 \\ C_{n_{\delta_a}} b/t & 0 \end{bmatrix}.$$

B. Dynamics equations

The dynamics equations of the actuated paraglider are obtained by combining the free dynamics (5) and the aerodynamics variation due to the flaps (6):

$$A \begin{bmatrix} \dot{V}_{cm} \\ \dot{\omega} \end{bmatrix} = B + Su_\delta \tag{7}$$

where

$$A = \begin{bmatrix} M+M_F & 0 \\ R_{gc}M_F & I+I_F \end{bmatrix}$$

$$B = \begin{bmatrix} W+F_A^c+F_A^b-\Omega M_F V_c-(M+M_F)\Omega V_{cm} \\ M_A^c-\Xi_c M_F V_c+R_{gc}(F_A^c-\Omega M_F V_c)+ \\ +R_{gb}F_A^b-\Omega(I+I_F)\omega \end{bmatrix}$$

$$S = \frac{1}{2}\rho S_c\|V_c\|^2 \begin{bmatrix} S_{F_a^c} \\ S_{M_a^c}+R_{gc}S_{F_a^c} \end{bmatrix}$$

$$u_\delta = \begin{bmatrix} \delta_a & \delta_s \end{bmatrix}^T.$$

A is always non singular, thus it can be inverted obtaining

$$\begin{bmatrix} \dot{V}_{cm} \\ \dot{\omega} \end{bmatrix} = f(V_{cm},\omega)+g(V_{cm},\omega)u_\delta. \tag{8}$$

C. A simplified model

For the purpose of control design and stability analysis, a simplified model has been developed, by neglecting: (*i*) apparent mass and inertia effects which become negligible near steady-state conditions; (*ii*) moments of aerodynamic forces on the CM which are smaller than the aerodynamic rolling, pitching and yawing moments; (*iii*) payload drag which is proportional to the surface and therefore much smaller than the parafoil drag; (*iv*) the contribution to the velocity of the parafoil due to the different location of the center of pressure of the parafoil and the center of mass (i.e., the velocity of the parafoil is considered to be the same as the velocity of the CM). These are common assumptions in the control of parafoil-payload systems [15].

The dynamics of the system becomes

$$M\dot{V}_{cm} = W+F_A^c+-M\Omega V_{cm}+S_{F_a^c}u$$
$$I\dot{\omega} = M_A^c-\Omega I\omega+S_{M_a^c}u. \tag{9}$$

Defining lift $L=\frac{1}{2}\rho S_c V_T^2 C_L$ and drag $D=\frac{1}{2}\rho S_c V_T^2 C_D$, eq. (9) are written in the explicit form as:

$$\dot{V}_T = g\left(-s_\vartheta c_\alpha c_\beta+s_\varphi c_\vartheta s_\beta+c_\varphi c_\vartheta s_\alpha c_\beta\right)+$$
$$- \frac{D}{m}-\frac{1}{2m}\rho V_T^2 S_c C_{D_\delta}\delta_s$$

$$\dot{\alpha} = \frac{g}{V_T}\left(s_\vartheta t_\alpha+c_\varphi c_\vartheta\right)+q\frac{c_\beta}{c_\alpha}-\frac{s_\beta}{c_\alpha}\left(pc_\alpha+rs_\alpha\right)+$$
$$- \frac{L}{mV_T}\frac{c_\beta}{c_\alpha}-\frac{1}{2m}\rho V_T S_c C_{L_\delta}\frac{c_\beta}{c_\alpha}\delta_s$$

$$\dot{\beta} = \frac{g}{V_T}\left(s_\vartheta c_\alpha s_\beta+s_\varphi c_\vartheta c_\beta-c_\varphi c_\vartheta s_\alpha s_\beta\right)+ps_\alpha-rc_\alpha$$

$$\dot{p} = \frac{1}{4I_{xx}}\rho S_c V_T\left(C_{l_p}b^2 p+2C_{l_\varphi}b\varphi V_T\right)+qr\frac{I_{zz}-I_{yy}}{I_{xx}}+$$
$$+ \frac{1}{2I_{xx}}\rho S_c V_T C_{l_\delta}\frac{b}{t}\delta_a$$

$$\dot{q} = \frac{1}{4I_{yy}}\rho S_c V_T\left(C_{m_q}c^2 q+2C_m cV_T\right)+pr\frac{I_{xx}-I_{zz}}{I_{yy}}$$

$$\dot{r} = \frac{1}{4I_{zz}}\rho S_c V_T\left(C_{n_r}b^2 r\right)+pq\frac{I_{yy}-I_{xx}}{I_{zz}}+$$
$$+ \frac{1}{2I_{zz}}\rho S_c V_T^2 C_{n_\delta}\frac{b}{t}\delta_a.$$

III. THE PATH FOLLOWING ALGORITHM

The path following problem addressed in this paper can be formulated as follows. The inertial coordinates x,y of the paraglider's CM must reach a linear path in the XY plane and follow it with the heading ψ aligned with the path slope ψ_{ref}, starting from a given initial configuration (on or off the path). Without loss of generality, the linear path can be considered to be coincident with the X axis of the inertial reference frame. The line following problem then reduces to the stabilization of the state variables y and ψ to zero.

By virtue of the above formulation, the path following problem is not affected by the x,z coordinates nor they influence the internal stability of the system. They can therefore be left out of the following analysis in which we show that local stabilization of an appropriate equilibrium point solves the considered path following problem.

Considering the simplified model (9) and the kinematic equations (1), the system motion can be described in terms of lateral and reduced longitudinal dynamics respectively associated to the state variables $\zeta_{lat} = [y,\varphi,\psi,\beta,p,r]^T$ and $\zeta_{long} = [\vartheta,V_T,\alpha,q]^T$.

We will show in what follows that a stable line following in the XY plane can be achieved by setting $\delta_s=0$ and using only δ_a as a control input. The use of a $\delta_s\neq 0$ produces, in fact, unnecessary (w.r.t. the considered problem) height loss, thus reducing the time of flight before landing.

The reduced model considered for control design and stability analysis is therefore:

$$\dot{\zeta}_{lat} = f_{lat}(\zeta_{lat},\zeta_{long})+g_{lat}(\zeta_{long})\delta_a \tag{10}$$
$$\dot{\zeta}_{long} = f_{long}(\zeta_{lat},\zeta_{long}),$$

with obvious definition of $f_{lat/long}$ and g_{lat}.

The unforced equilibrium of system (10) considered in the following is $\zeta_{lat}^e = [0,0,0,0,0,0]^T$ and $\zeta_{long}^e = [\vartheta^e,V_T^e,\alpha^e,0]^T$, where the equilibrium values $[\vartheta^e,V_T^e,\alpha^e]$ are computed by solving the equation $f_{long}(0,\zeta_{long}^e)=0$ admitting the unique feasible solution

$$\vartheta^e = \alpha^e-\text{atan}\left(\frac{C_{D_0}+C_{D_\alpha}(\alpha^e)^2}{C_{L_0}+C_{L_\alpha}\alpha^e}\right)$$

$$V_T^e = \sqrt{\frac{2mg\sin(\alpha^e-\vartheta^e)}{\rho S_c\left(C_{D_0}+C_{D_\alpha}(\alpha^e)^2\right)}}$$

$$\alpha^e = -\frac{C_{m_0}}{C_{m_\alpha}}.$$

Being $\vartheta\in(-\pi/2,\pi/2)$ and $\alpha^e-\vartheta^e=\text{atan}(1/E)$, where $E=L/D>1$ is the parafoil's efficiency, it follows that $0<\alpha^e-\vartheta^e<\pi/4$. Such a condition assures the feasibility of the equilibrium state ζ_{long}^e because $\sin(\alpha^e-\vartheta^e)>0$, thus V_T^e is real. Moreover, only the solution $V_T^e>0$ is admissible.

The control objective thus reduces to enducing asymptotic stability of the equilibrium $\zeta^e = [\zeta_{lat}^e,\zeta_{long}^e]$ via feedback. Note that this equilibrium point belongs to the manifold defined by the dynamics of the state variables β,φ,p,r. which turns out to be structurally stable since its linear approximation around the equilibrium point $\zeta_{long}=\zeta_{long}^e$ and

$[\beta, \varphi, p, r]^T = [0,0,0,0]^T$ is decoupled from the longitudinal motion and characterized by the eigenvalues

$$\lambda_1 = \frac{mg\sin(\vartheta^e - \alpha^e)}{V_T^e} \qquad \lambda_2 = \frac{1}{4}\frac{\rho S_c V_T^e C_{n_r}}{I_{zz}}$$

$$\lambda_3 = \frac{1}{8}\frac{\left(C_{l_p}S_c\rho b^2 + \sqrt{C_{l_p}^2 S_c^2\rho^2 b^4 + 32 I_{xx}C_{l_\varphi}S_c\rho b}\right)V_T^e}{I_{xx}}$$

$$\lambda_4 = \frac{1}{8}\frac{\left(C_{l_p}S_c\rho b^2 - \sqrt{C_{l_p}^2 S_c^2\rho^2 b^4 + 32 I_{xx}C_{l_\varphi}S_c\rho b}\right)V_T^e}{I_{xx}}.$$

These are in the left-half plane since $\vartheta^e - \alpha^e < 0$ and the aerodynamic coefficients C_{l_φ}, C_{l_p} and C_{n_r} are negative, being the damping terms of the lateral dynamics.

The projection on the XY plane of the corresponding system trajectories are straight lines with equilibrium values of y and ψ depending on the initial state of the system.

A. Control design and stability analysis

To attack the line following problem defined above, we first feedback linearize system (10) with respect to the output

$$h = y + \psi. \qquad (11)$$

The system relative degree associated to output (11) w.r.t. the input δ_a is 2, being

$$\ddot{h} = \ddot{y} + \frac{\dot{\varphi}\dot{\vartheta}}{c_\vartheta} + t_\vartheta\dot{\vartheta}\dot{\psi} + \frac{s_\varphi}{c_\vartheta}\dot{q} + \frac{c_\varphi}{c_\vartheta}(f_r + g_r\delta_a)$$

where, according to eq. (10), the dynamics of r has been written as $\dot{r} = f_r + g_r\delta_a$ to make the dependance on the input δ_a explicit. The input-output feedback linearizing control is readily found to be:

$$\delta_a = \frac{c_\vartheta}{c_\varphi g_r}\left(v - \ddot{y} - \frac{\dot{\varphi}\dot{\vartheta} + s_\vartheta\dot{\vartheta}\dot{\psi}}{c_\vartheta} - \frac{s_\varphi}{c_\vartheta}\dot{q} - \frac{c_\varphi}{c_\vartheta}f_r\right), \quad (12)$$

being v the new control input.

To show that, with an appropriate choice of v, this control law locally asymptotically stabilizes the equilibrium ζ^e, it is convenient to put the system in normal form [16]. Consider therefore the mapping

$$\begin{array}{llll} z_1 &= y + \psi & z_3 &= \beta \\ z_2 &= \dot{y} + \dot{\psi} & z_4 &= \varphi \\ & & z_5 &= p \\ & & z_6 &= \psi \end{array}, \qquad (13)$$

involving only the state variables characterizing the lateral dynamics. It is easily verified that the jacobian matrix determinant Δ_Φ of the mapping Φ, formed by (13) and the identity mapping relative to the longitudinal dynamics variables ζ_{long}, is $\Delta_\Phi = -\dfrac{\cos(\varphi)}{\cos(\vartheta)}$. This determinant is never zero for admissible values of the state variables and therefore Φ qualifies as a coordinate transformation.

By choosing $v = -K_p z_1 - K_d z_2$, with gains $K_p > 0$ and $K_d > 0$, the closed loop dynamics of system (10) in the new coordinates can be written as

$$\begin{array}{lll} \dot{\xi} &=& A_\xi\xi \\ \dot{\eta}_{lat} &=& f_{\eta_{lat}}(\xi, \eta_{lat}, \eta_{long}) \\ \dot{\eta}_{long} &=& f_{\eta_{long}}(\xi, \eta_{lat}, \eta_{long}) \end{array} \qquad (14)$$

where

$$\xi = \begin{bmatrix} z_1 \\ z_2 \end{bmatrix}, \quad A_\xi = \begin{bmatrix} 0 & 1 \\ -K_p & -K_d \end{bmatrix}$$

$$\eta_{lat} = \begin{bmatrix} z_3 & \cdots & z_6 \end{bmatrix}^T \quad \eta_{long} = \zeta_{long}.$$

Defining

$$F_{lat} = \left[\frac{\partial f_{\eta_{lat}}(\xi, \eta_{lat}, \eta_{long})}{\partial \eta_{lat}}\right]_{(\xi, \eta_{lat}, \eta_{long})=(0,0,\zeta_{long}^e)}$$

$$F_{long} = \left[\frac{\partial f_{\eta_{long}}(\xi, \eta_{lat}, \eta_{long})}{\partial \eta_{long}}\right]_{(\xi, \eta_{lat}, \eta_{long})=(0,0,\zeta_{long}^e)},$$

it is easy to verify that the linear approximation of (14) around the equilibrium $(0,0,\zeta_{long}^e)$ takes the form

$$\begin{bmatrix} \dot{\xi} \\ \dot{\eta}_{lat} \\ \dot{\eta}_{long} \end{bmatrix} = \begin{bmatrix} A_\xi & 0 & 0 \\ \star & F_{lat} & 0 \\ 0 & 0 & F_{long} \end{bmatrix} \begin{bmatrix} \xi \\ \eta_{lat} \\ \eta_{long} - \zeta_{long}^e \end{bmatrix}.$$

The local stability of the considered paraglider can be verified by computing the eigenvalues of F_{lat} and F_{long} for the parameters' values reported in Table I and II. Therefore, under the chosen control law we have that both $z_1 = y + \psi$ and $z_6 = \psi$ locally exponentially converge to zero and thus also y converges to zero as required in the problem formulation.

TABLE I

PHYSICAL CHARACTERISTICS OF THE MULTIBODY SYSTEM

	Payload	Parafoil
Mass [kg]	135	13
Geometry [m]	0.5 × 0.5 × 0.5	7 × 3 × 0.3 [b × c × t]
Surface [m^2]	1.5	21
Distance from joint [m]	0.5	7.5

TABLE II

PARAFOIL AND PAYLOAD AERODYNAMIC COEFFICIENTS

C_{L_0}	0.4	C_{L_α}	2	$C_{L_{\delta_s}}$	0.21
C_{D_0}	0.15	C_{D_α}	1	$C_{D_{\delta_s}}$	0.3
C_{m_0}	0.018	C_{m_α}	-0.2	C_{m_q}	-2
C_{l_φ}	-0.05	C_{l_p}	-0.1	$C_{l_{\delta_a}}$	0.0021
-	-	C_{n_r}	-0.07	$C_{n_{\delta_a}}$	0.004

IV. SIMULATION RESULTS

The proposed line tracking algorithm has been validated through simulations. Two different path following tasks have been considered: a pure line and a polygonal path. In both simulations the feedback variable y was weighted by a positive factor w_y to account for the different physical nature of y and ψ (linear *vs.* angular quantities), achieving a similar control authority on both the control variables. The PD gains are $K_p = 0.2$ and $K_d = 2$ while the weight is $w_y = 0.01$.

In the first simulation, the reference path is represented by the X axis of the inertial reference frame. We compare the system's closed-loop behavior when the control input (12) is applied to either the simplified model of eq. (9) or the complete dynamics of eq. (8). This comparison allows validating the local stability result.

The paraglider starts from inertial coordinates $(0, 10, -1500)$ m, with a velocity of 10 m/s and angle of attack of $8°$, while the sideslip angle is zero. Euler angles and angular velocities are initially zeros. The system reaches the desired reference line with a transient shaped by the gain values. Figure 2 shows the path in the XY plane followed by the paraglider with both models. Despite the transient oscillating behavior, convergence rate and tracking accuracy of the two dynamics are comparable.
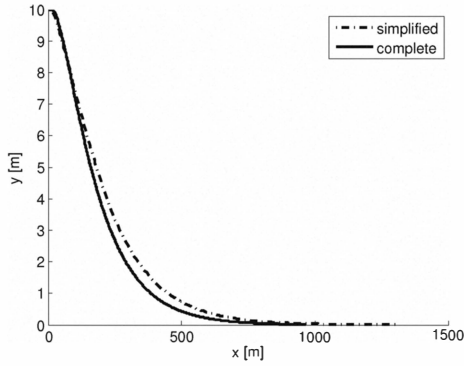
Fig. 2.   XY path

At steady-state, the Euler angles reach the equilibrium values $\varphi = \psi = 0$ and $\theta = \theta_e$, this last being different whether the simplified or the complete dynamics is considered, as shown in Fig. 3. Angular velocities converge to zero, as well as the sideslip angle β, while V_T and α converge to their equilibrium values that depend on the dynamics (simplified or complete), see Fig. 4 and 5.
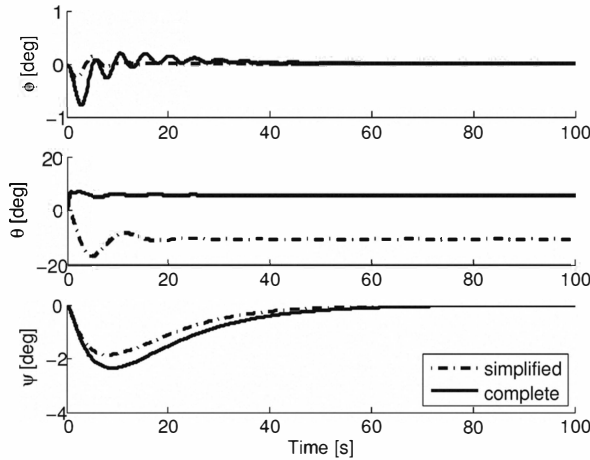

Fig. 3.   Euler angles time history

The evolution of the control input δ_a is plotted in Fig. 6. During the transient, the control reaches its maximum am-
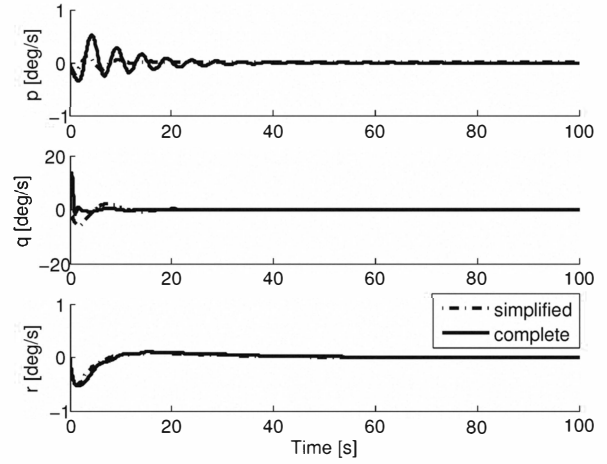

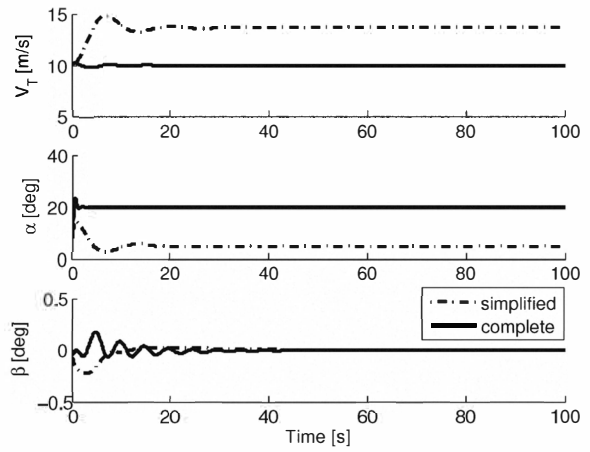Fig. 4.   Angular velocities time history

Fig. 5.   Velocity components

plitude, about $8°$, while it converges to zero as soon as the system is on the reference line with the heading angle parallel to the path, as shown in Fig. 3.
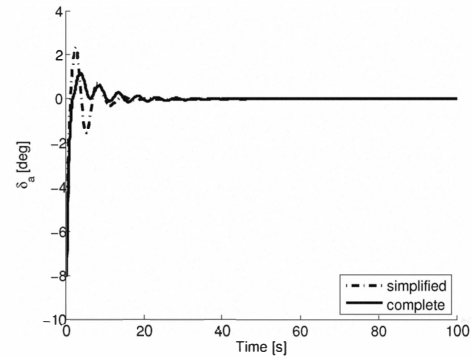

Fig. 6.   Asymmetric control

To further evaluate the performance of the proposed controller, a segmented reference path is considered and the proposed control law is simulated with the complete dynamics of eq. (8).

4873

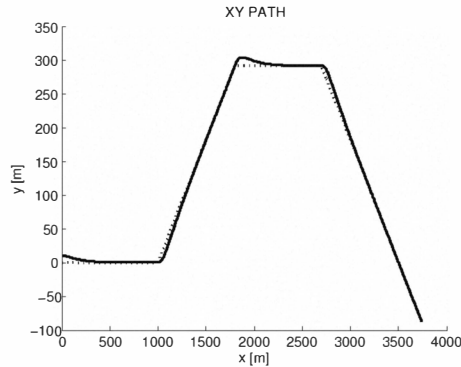Figure 7 shows the travelled *vs.* the desired path.

Fig. 7.   XY path for segmented reference path

The path error converges to zero for each segment in about 50 *s*, as the heading angle goes to the reference value, which is zero when the line is parallel to the X axis and is $\pm 20°$ for the slanted lines. Performance is shown in Fig. 8, where the path error and the heading angle error are plotted.
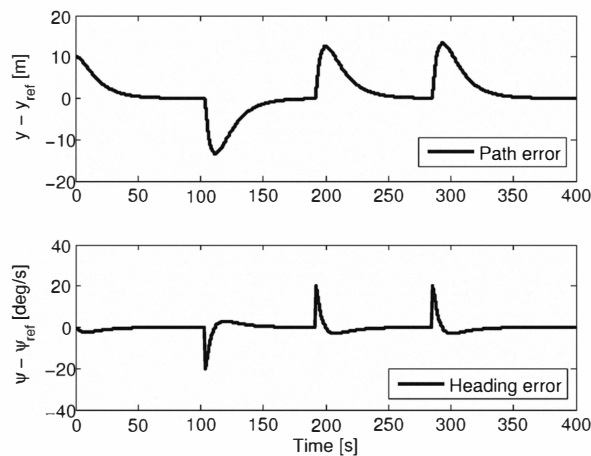

Fig. 8.   Upper plot: path error. Lower plot: heading angle error

The asymmetric control time history is plotted in Fig. 9. Despite the presence of spikes corresponding to path slope changes, the control input is always within the admissible range $\pm 90°$.

V. CONCLUSIONS

A control algorithm for autonomous paragliders has been proposed for linear path following. A 6-DOF model is used to describe the dynamics, accounting for weight, aerodynamic forces on payload and parafoil, aerodynamic moments, effect of apparent forces and moments, moments generated on the center of mass by the forces exerted at the payload and parafoil. Local exponential stability of the input-output feedback linearizing and stabilizing control has been proved and a stable line following in the XY plane has been achieved by using only the lateral directional control input.

Future work will focus on formulating a path following algorithm for curve paths and using also the longitudinal directional control input δ_s to enhance performance.
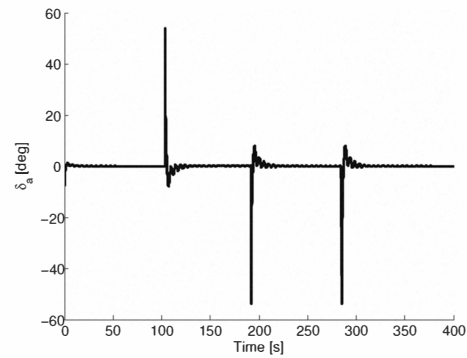

Fig. 9.   Asymmetric control for segmented reference path

REFERENCES

[1] M. Canale, L. Fagiano, M. Ippolito and M. Milanese, "Control of tethered airfoils for a new class of wind energy generator," *in 45th IEEE Conference on Decision and Control*, San Diego, CA, USA, 2006.
[2] H. G. Heinrich and L. W. Rust, Jr., "Dynamic Stability of a System consisting of a Stable Parachute and an Unstable Load," Technical Report No. AFFDL-TR64-194, University of Minnesota, 1965.
[3] D. Wolf, "Dynamic Stability of a Nonrigid Parachute and Payload System," PhD Thesis, University of Rhode Island, 1968.
[4] P.B.S. Lissaman and G.J. Brown, "Apparent Mass Effects on Parafoil Dynamics," AIAA-93-1236, 1993.
[5] C. Schroeder Iacomini and C.J. Cerimele, "Lateral-Directional Aerodynamics from a Large Scale Parafoil Test Program," AIAA-99-1731, 1999.
[6] C. Schroeder Iacomini and C.J. Cerimele, "Longitudinal Aerodynamics from a Large Scale Parafoil Test Program," AIAA-99-1732, 1999.
[7] P. V. Zaitsev and A. M. Formal'skii, "Autonomous Longitudinal Motion of a Paraglider. Mathematical Simulation, Synthesis of Control," *Journal of Computer and Systems Sciences International*, Vol. 47, No. 5, pp. 786–794, 2008.
[8] T. Jann, "Aerodynamic Model Identification and GNC Design for the Parafoil-Load System ALEX," AIAA-2001-2015, 2001.
[9] N. Slegers, E. Beyer and M. Costello, "Use of Variable Incidence Angle for Glide Slope Control of Autonomous Parafoils," *Journal of Guidance, Control and Dynamics*, Vol. 31, No. 3, pp. 585–596, 2008.
[10] S. Müller, O. Wagner, and G. Sachs, "A High-Fidelity Nonlinear Multibody Simulation model for Parafoil Systems," AIAA-2003-2120, 2003.
[11] C. Redelinghuys, "A Flight Simulation Algorithm for a Parafoil Suspending an Air Vehicle," *Journal of Guidance, Control and Dynamics*, Vol. 30, No. 3, pp. 791–803, 2007.
[12] N. Slegers, "Effects of Canopy-Payload Relative Motion on Control of Autonomous Parafoils," *Journal of Guidance, Control and Dynamics*, Vol. 33, No. 1, pp. 116–126, 2010.
[13] N. Slegers and M. Costello, "Aspects of Control for a Parafoil and Payload System," *Journal of Guidance, Control and Dynamics*, Vol. 26, No. 6, pp. 898–905, 2003.
[14] N. Slegers and O. Yakimenko, "Optimal Control for Terminal Guidance of Autonomous Parafoils," AIAA 2009-2958, 2009.
[15] N. Slegers, J. Kyle, M. Costello, "Nonlinear Model Predictive Control Technique for Unmanned Air Vehicles," *Journal of Guidance, Control, and Dynamics*, Vol. 29, No. 5, pp. 1179–1188, 2006.
[16] A. Isidori, "Nonlinear Control Systems," Springer-Verlag, New York, 1989.